Fundamental Problems in Subatomic Physics 2026

Production of High-Orbital Kaon Excited States in the K−p reaction

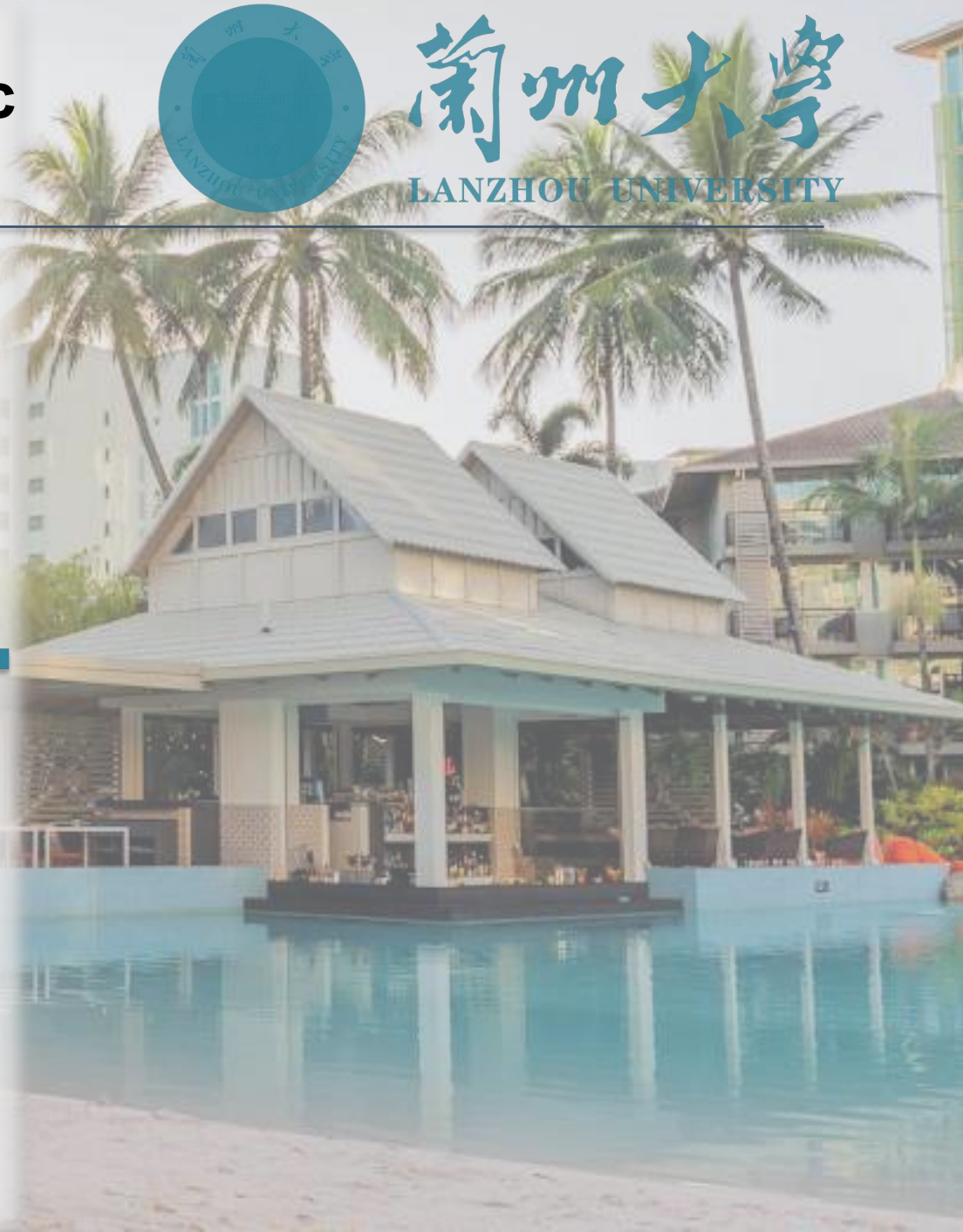
Ting-Yan Li (李亭彦)

with Zi-Yue Bai (白紫跃) and Xiang Liu (刘翔)

School of Physical Science and Technology, Lanzhou University

23–27 September 2026 · Cairns, Australia

Phys.Rev.D 114 (2026) 3, 034049 · lity2023@lzu.edu.cn



OUTLINE

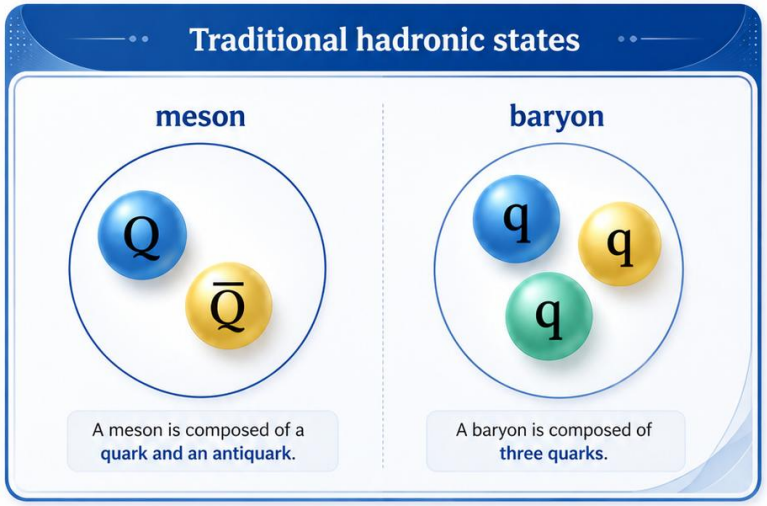
01 BACKGROUND & MOTIVATION

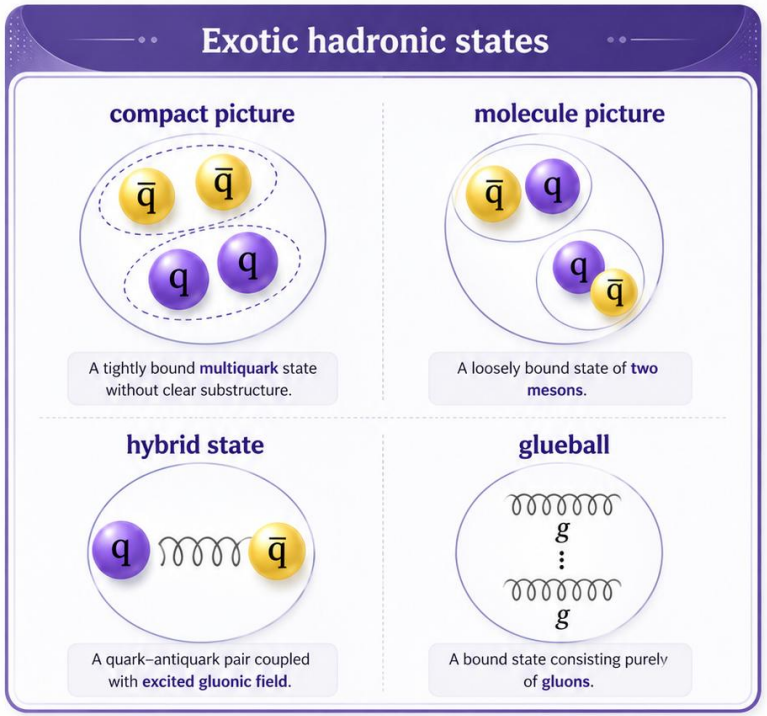
02 THEORETICAL FRAMEWORK

03 NUMERICAL RESULTS

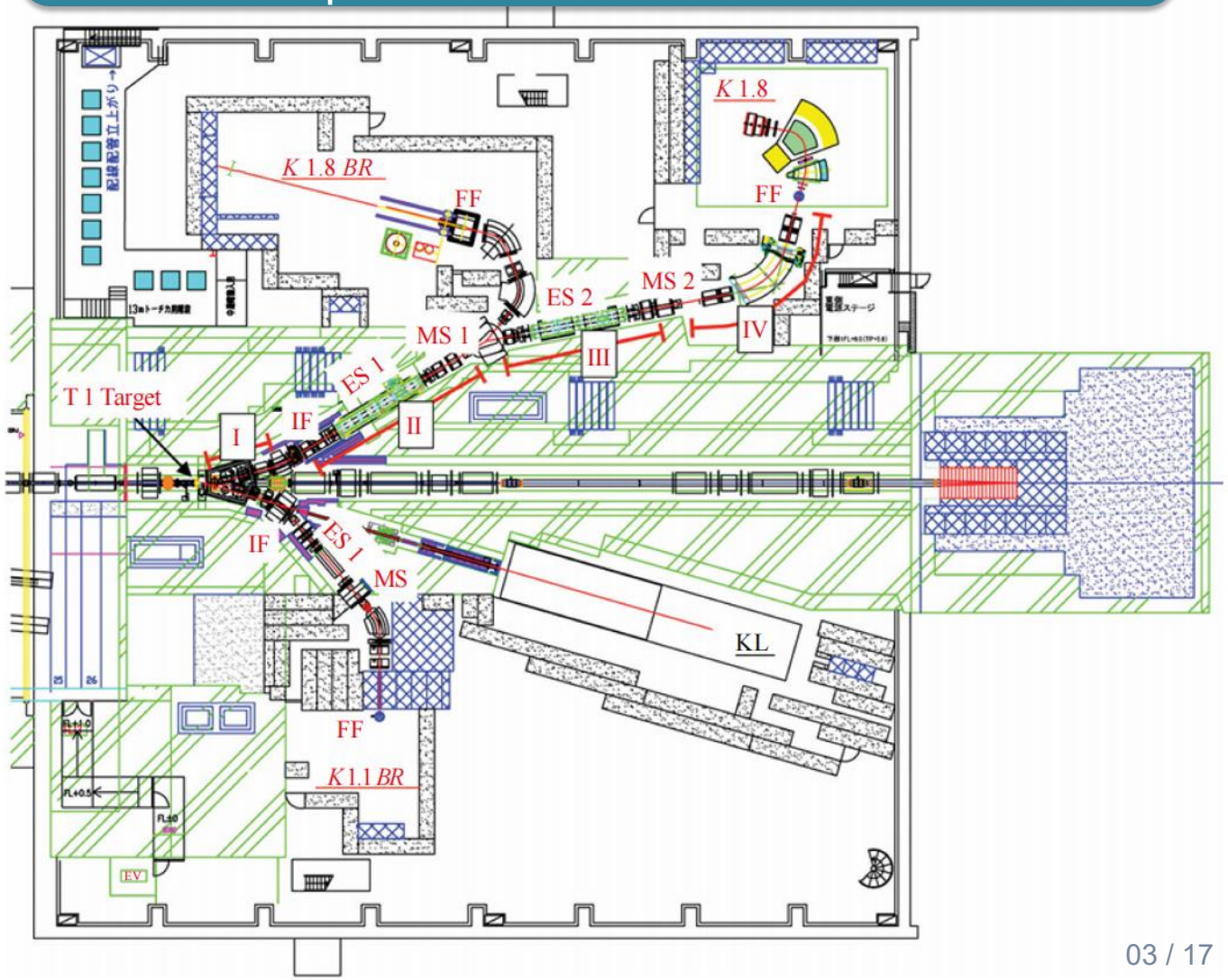
04 OUTLOOK

Meson beam experiments





Layout diagrams of the Hadron Experimental Hall, charged secondary beamlines, and various experimental areas at J-PARC



Light hadrons measured by meson beam experiments

Table 1. Light-Meson Spectrum Listed in the PDG [5] (Check-Marked Particles Have Been Measured in Molecular-Beam Experiments)

Particle	J^P	Molecular-Beam Experiment	Particle	J^P	Molecular-Beam Experiment	Particle	J^P	Molecular-Beam Experiment	Particle	J^P	Molecular-Beam Experiment
η	0^-	✓	$\rho(1450)$	1^-		$\eta_2(1870)$	2^-	✓	$\rho_5(2350)$	5^-	✓
f_0(500)	0^+		$\eta(1475)$	0^-	✓	$\pi_2(1880)$	2^-		$f_6(2510)$	6^+	✓
$\rho(770)$	1^-	✓	$f_0(1500)$	0^+	✓	$\rho(1900)$	1^-		$K_0^*(700)$	0^+	✓
$\omega(782)$	1^-	✓	$f_1(1510)$	1^+	✓	$f_2(1910)$	2^+	✓	$K^*(892)$	1^-	✓
$\eta'(958)$	0^-	✓	$f_2'(1525)$	2^+	✓	$a_0(1950)$	0^+		$K_1(1270)$	1^+	✓
$f_0(980)$	0^+	✓	$f_2(1565)$	2^+	✓	$f_2(1950)$	2^+	✓	$K_1(1400)$	1^+	✓
$a_0(980)$	0^+	✓	$\rho(1570)$	1^-	✓	$\rho_3(1990)$	3^-		$K^*(1410)$	1^-	✓
$\phi(1020)$	1^-	✓	$h_1(1595)$	1^+	✓	$\pi_2(2005)$	2^-	✓	$K_0^*(1430)$	0^+	✓
$h_1(1170)$	1^+	✓	$\pi_1(1600)$	1^-	✓	$f_2(2010)$	2^+	✓	$K_2^*(1430)$	2^+	✓
$b_1(1235)$	1^+	✓	$a_1(1640)$	1^+	✓	$f_0(2020)$	0^+	✓	$K(1460)$	0^-	✓
$a_1(1260)$								✓	$K_2(1580)$	2^-	✓
$f_2(1270)$								✓	$K(1630)$	?	✓
$f_1(1285)$	1^+	✓	$\omega(1650)$	1^-		$\pi_2(2100)$	2^-	✓	$K_1(1650)$	1^+	✓
$\eta(1295)$	0^-		$\omega_3(1670)$	3^-	✓	$f_0(2100)$	0^+		$K^*(1680)$	1^-	✓
$\pi(1300)$	0^-		$\pi_2(1670)$	2^-	✓	$f_2(2150)$	2^+	✓	$K_2(1770)$	2^-	✓
$a_2(1320)$	2^+	✓	$\phi(1680)$	1^-		$\rho(2150)$	1^-		$K_3^*(1780)$	3^-	✓
$f_0(1370)$	0^+		$\rho_3(1690)$	3^-	✓	$\phi(2170)$	1^-		$K_2(1820)$	2^-	✓
$h_1(1380)$	1^+		$\rho(1700)$	1^-	✓	$f_0(2200)$	0^+	✓	$K(1830)$	0^-	✓
$\pi_1(1400)$	1^-	✓	$a_2(1700)$	2^+	✓	$f_J(2220)$	$2^+, 4^+$		$K_0^*(1950)$	0^+	✓
$\eta(1405)$	0^-	✓	$f_0(1710)$	0^+	✓	$\eta(2225)$	0^-		$K_2^*(1980)$	2^+	✓
$f_1(1420)$	1^+	✓	$\eta(1760)$	0^-		$\rho_3(2250)$	3^-	✓	$K_4^*(2045)$	4^+	✓
$\omega(1420)$	1^-		$\pi(1800)$	0^-	✓	$f_2(2300)$	2^+	✓	$K_2(2250)$	?	✓
$a_1(1420)$	1^+	✓	$f_2(1810)$	2^+	✓	$f_4(2300)$	4^+		$K_3(2320)$	3^+	✓
$f_2(1430)$	2^+	✓	$X(1835)$	0^-		$f_0(2330)$	0^+		$K_5^*(2380)$	5^-	✓
$a_0(1450)$	0^+	✓	$\pi_3(1850)$	3^-	✓	$f_2(2340)$	2^+		$K_4(2500)$	4^-	✓

So many mesons measured by meson beam experiments!

Low-spin

High-spin

High-orbital kaons

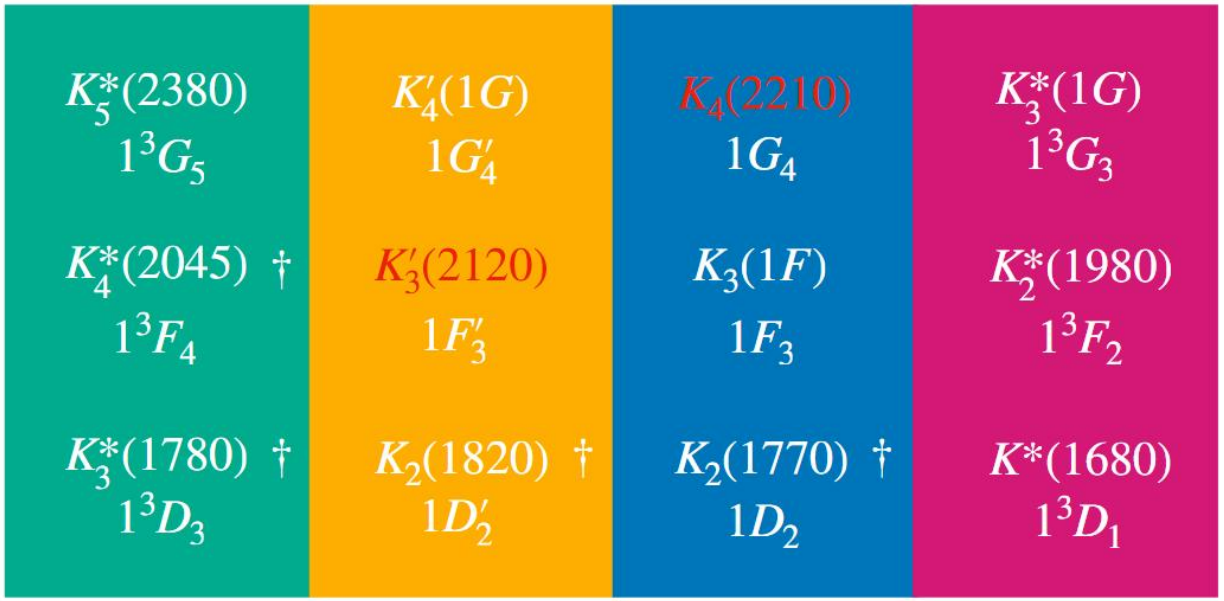


FIG. 1: A collection of high-orbital kaons. Two newly observed kaons, $K_3'(2120)$ and $K_4(2210)$, are marked in red, as reported by the COMPASS Collaboration in 2025 [13]. Four states marked with asterisks have corresponding experimental cross-section data available for $K^- p$ reactions.

TABLE I: Summary of the high-orbital kaon states considered in this work. The labels $1L_J$ and $1L_J'$ denote the two physical states arising from the mixing of the 1^1L_J and 1^3L_J configurations.

	States	J^P	$n^{2S+1}L_J$	Status	Assignment
$1D$	$K_3^*(1780)$	3^-	1^3D_3	Established	$q\bar{q}$ meson
	$K_2(1770)$	2^-	$1D_2$	Established	
	$K_2(1820)$	2^-	$1D_2'$	Established	
	$K^*(1680)$	1^-	1^3D_1	Established	
$1F$	$K_4^*(2045)$	4^+	1^3F_4	Established	$q\bar{q}$ meson
	$K_3'(2120)$	3^+	$1F_3'$	Candidate	
	$K_3(1F)$	3^+	$1F_3$	Predicted	
	$K_2^*(1980)$	2^+	1^3F_2	Candidate	
$1G$	$K_5^*(2380)$	5^-	1^3G_5	Candidate	$q\bar{q}$ meson
	$K_4(2210)$	4^-	$1G_4$	Candidate	
	$K_4'(1G)$	4^-	$1G_4'$	Predicted	
	$K_3^*(1G)$	3^-	1^3G_3	Predicted	

Phys.Rev.D 114 (2026) 3, 034049

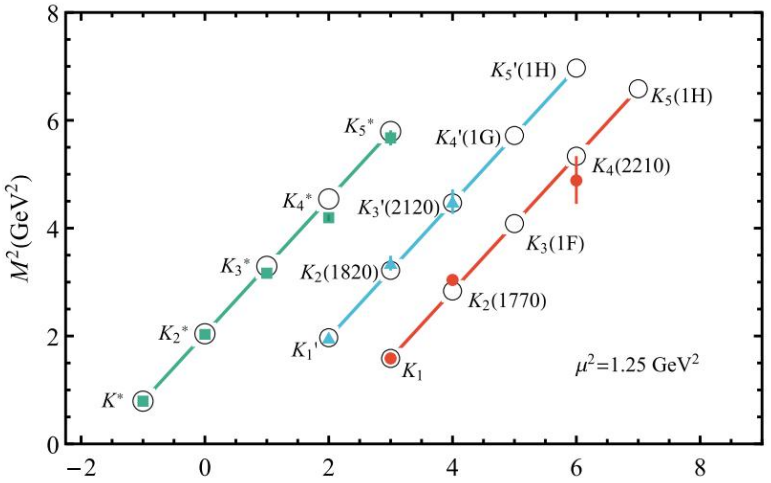
Meson spectroscopy and strong decay for high-orbital kaons

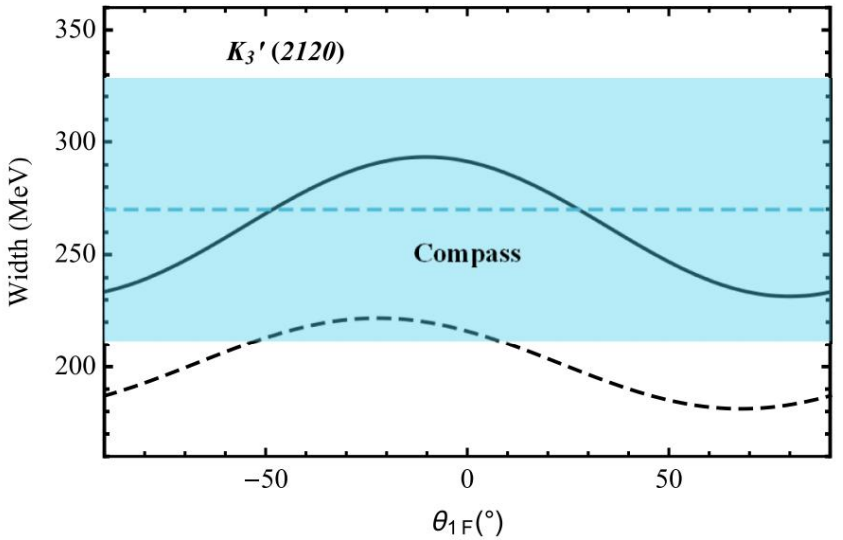
TABLE II. The mass spectrum of the high spin kaons. The results of "this work" do not take into account spin-mixing. The unit of mass is MeV. "Exp." represents the experimental value.

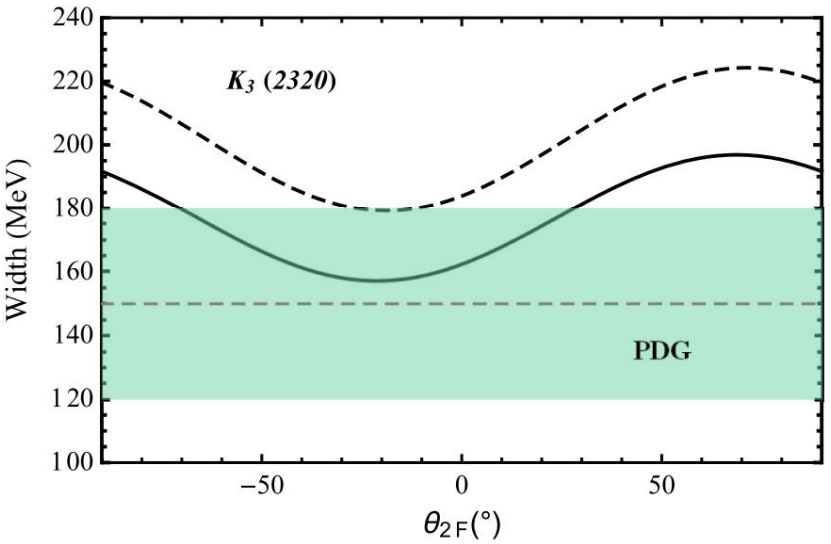
States	J^P	$n^{2S+1}L_J$	This work	GI [57]	Segovia [9]	Ebert [3]	Exp.
$K_3(1F)$	3^+	1^1F_3	2066	2130	2047	2009	···
$K_3'(2120)$	3^+	1^3F_3	2064	2146	2132	2080	$2119 \pm 13^{+45}_{-12}$ [1]
$K_3^*(1780)$	3^-	1^3D_3	1794	1780	1810	1789	1779 ± 8 [11]
$K_3(2320)$	3^+	2^1F_3	2347	2524	2340	2384	2324 ± 24 [11]
$K_3'(2F)$	3^+	2^3F_3	2347	2539	2387	···	···
$K_4(2210)$	4^-	1^1G_4	2307	2422	2270	2255	$2210 \pm 40^{+80}_{-30}$ [1]
$K_4'(1G)$	4^-	1^3G_4	2306	2435	2337	2285	···
$K_4^*(2045)$	4^+	1^3F_4	2075	2097	2080	2096	$2060 \pm 5^{+11}_{-3}$ [1], 2048^{+8}_{-9} [11]
$K_4(2500)$	4^-	2^1G_4	2538	2778	2476	2575	2490 ± 20 [11]
$K_4'(2G)$	4^-	2^3G_4	2538	2790	2510	···	···
$K_5(1H)$	5^+	1^1H_5	2509	2682	2442	···	···
$K_5'(1H)$	5^+	1^3H_5	2509	2693	2489	···	···
$K_5^*(2380)$	5^-	1^3G_5	2309	2379	2291	···	2382 ± 24 [11]

TABLE III. The decay information of $K_3^*(1780)(1^3D_3)$. The unit of the width is MeV. The abbreviation "Br" denotes the branching ratio. The data in {} means the width calculated using the theoretical mass of the initial state.

Channel	Br (%)	Exp. [11]	Value
ρK^*	43.2{44.3}	···	48.7{57.8}
ωK^*	13.4{14.0}	···	15.1{18.2}
πK	12.8{11.7}	0.188 ± 0.01	14.4{15.3}
πK^*	10.5{9.99}	0.2 ± 0.05	11.8{13.0}
$K\rho$	8.51{8.27}	0.31 ± 0.09	9.59{10.8}
$K\eta$	4.26{4.02}	0.3 ± 0.13	4.8{5.25}
$K\omega$	2.73{2.66}	···	3.08{3.47}
πK_2^*	1.35{1.53}	< 0.16	1.52{2}
πK_1	1.29{1.32}	···	1.45{1.72}
		···	
Total	100{100}	161 ± 17	113{130}

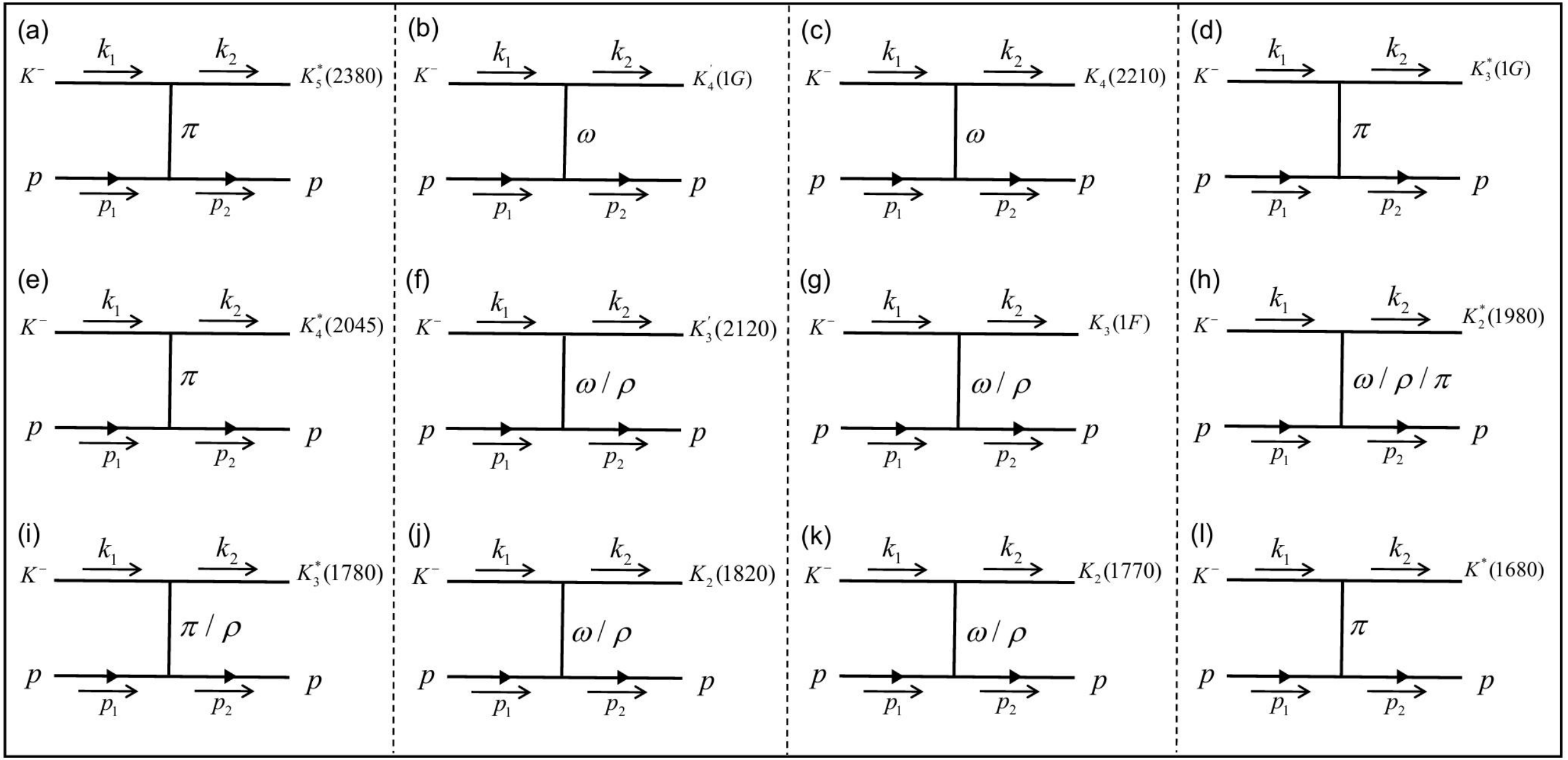






The establishment of the kaon meson family remains to be improved

The effective Lagrangian approach



Feynman diagrams for the K + p → K_J + N reactions.

Representative effective interactions

High-spin upper vertex

$$\mathcal{L}_{K_3^*(1780)K\pi} = g_{K_3^*(1780)K\pi} K_3^{*+,\mu\nu\rho} \Big[K^- (\partial_\mu\partial_\nu\partial_\rho\pi^0) - \pi^0 (\partial_\mu\partial_\nu\partial_\rho K^-)\Big],$$

$$\mathcal{L}_{K_2(1820)\omega K} = g_{K_2(1820)\omega K} K_2^{+,\alpha\beta} \omega_\alpha \partial_\beta K^-,$$

$$\mathcal{L}_{K_2(1770)\omega K} = g_{K_2(1770)\omega K} K_2^{+,\alpha\beta} \omega_\alpha \partial_\beta K^-,$$

$$\mathcal{L}_{K^*(1680)K\pi} = g_{K^*(1680)K\pi} K^{*0,\alpha} (K^-\partial_\alpha\pi^+ - \pi^+\partial_\alpha K^-).$$

$$\mathcal{L}_{K_4^*(2045)\pi K} = g_{K_4^*(2045)\pi K} K_4^{*+,\mu\nu\rho\sigma} \Big[K^-(\partial_\mu\partial_\nu\partial_\rho\partial_\sigma\pi^0) + \pi^0(\partial_\mu\partial_\nu\partial_\rho\partial_\sigma K^-)\Big].$$

$$\mathcal{L}_{K_3'(2120)\omega K} = g_{K_3'(2120)\omega K} K_3'^{+,\alpha\beta\gamma} \omega_\alpha \partial_\beta\partial_\gamma K^-,$$

$$\mathcal{L}_{K_3(1F)\omega K} = g_{K_3(1F)\omega K} K_3^{+,\alpha\beta\gamma} \omega_\alpha \partial_\beta\partial_\gamma K^-,$$

$$\mathcal{L}_{K_2^*(1980)\omega K} = g_{K_2^*(1980)\omega K} \varepsilon^{\mu\nu\lambda\sigma} K_{2,\mu\alpha}^{*+} (\partial_\nu\omega_\lambda)\partial_\sigma\partial^\alpha K^-,$$

$$\mathcal{L}_{K_2^*(1980)\pi K} = g_{K_2^*(1980)\pi K} K_2^{*+,\alpha\beta} \Big[K^-(\partial_\alpha\partial_\beta\pi^0) + \pi^0(\partial_\alpha\partial_\beta K^-)\Big].$$

$$\mathcal{L}_{K_5^*(2380)\pi K} = g_{K_5^*(2380)\pi K} K_5^{*+,\alpha\beta\gamma\delta\sigma} \Big[K^-(\partial_\alpha\partial_\beta\partial_\gamma\partial_\delta\partial_\sigma\pi^0) - \pi^0(\partial_\alpha\partial_\beta\partial_\gamma\partial_\delta\partial_\sigma K^-)\Big].$$

$$\mathcal{L}_{K_4'(1G)\omega K} = g_{K_4'(1G)\omega K} K_4'^{+,\alpha\beta\gamma\delta} \omega_\alpha \partial_\beta\partial_\gamma\partial_\delta K^-.$$

$$\mathcal{L}_{K_3^*(1G)\pi K} = g_{K_3^*(1G)\pi K} K_3^{*+,\alpha\beta\gamma} \Big[K^-(\partial_\alpha\partial_\beta\partial_\gamma\pi^0) - \pi^0(\partial_\alpha\partial_\beta\partial_\gamma K^-)\Big].$$

Vertices and amplitudes

πNN Vertex

$$\mathcal{L}_{\pi NN} = \frac{f_{\pi NN}}{m_\pi}\,\overline{N}\gamma_\mu\gamma^5\partial^\mu\tilde{\pi}\,N.$$

Vector VNN (V = ρ, ω)

$$\mathcal{L}_{\omega NN} = g_{\omega NN}\overline{N}\gamma_\mu\omega^\mu N + \frac{f_{\omega NN}}{4m_p}\overline{N}\sigma_{\mu\nu}\left(\partial^\mu\tilde{\omega}^\nu - \partial^\nu\tilde{\omega}^\mu\right)N,$$

$$\mathcal{L}_{\rho NN} = g_{\rho NN}\overline{N}\gamma_\mu\rho^\mu N + \frac{f_{\rho NN}}{4m_p}\overline{N}\sigma_{\mu\nu}\left(\partial^\mu\rho^\nu - \partial^\nu\rho^\mu\right)N.$$

Feynman amplitude

$$i\mathcal{M}_{K_3^*(1780)\pi K} = g_{K_3^*(1780)\pi K}\frac{f_{\pi NN}}{m_\pi}\bar{u}(p_2)\gamma_\alpha\gamma_5 u(p_1)\,q^\alpha\frac{i}{t-m_\pi^2} \times \epsilon^{*,\mu\nu\rho}(k_2)\left(q_\mu q_\nu q_\rho + k_{1\mu}k_{1\nu}k_{1\rho}\right)F_t(q). \quad (11)$$

$$i\mathcal{M}_{K_2(1820)\omega K} = i\,g_{K_2(1820)\omega K}\bar{u}(p_2)\left(g_{\omega NN}\gamma_\mu - \frac{if_{\omega NN}}{2m_p}\sigma_{\nu\mu}q^\nu\right)u(p_1) \times \epsilon^{*,\alpha\beta}(k_2)k_{1\beta}\frac{-i\left(g^\mu{}_\alpha + q^\mu q_\alpha/m_\omega^2\right)}{t-m_\omega^2}F_t(q). \quad (13)$$

$$i\mathcal{M}_{K_3'(2120)\rho K} = g_{K_3'(2120)\rho K}\bar{u}(p_2)\left(g_{\rho NN}\gamma_\mu - \frac{if_{\rho NN}}{2m_p}\sigma_{\nu\mu}q^\nu\right)u(p_1) \times \frac{-i\left(g^\mu{}_\alpha + q^\mu q_\alpha/m_\rho^2\right)}{t-m_\rho^2}\epsilon^{*,\alpha\beta\gamma}(k_2)k_{1\beta}k_{1\gamma}F_t(q). \quad (28)$$

$$i\mathcal{M}_{K_2^*(1980)\omega K} = -ig_{K_2^*(1980)\omega K}\varepsilon^{\mu\nu\lambda\sigma}\epsilon^*_{\mu\alpha}(k_2)q_\nu k_{1\sigma}k_1^\alpha \times \bar{u}(p_2)\left(g_{\omega NN}\gamma_\xi - \frac{if_{\omega NN}}{2m_p}\sigma_{\delta\xi}q^\delta\right)u(p_1) \times \frac{-i\left(g^\xi{}_\lambda + q^\xi q_\lambda/m_\omega^2\right)}{t-m_\omega^2}F_t(q), \quad (31)$$

Model parameter

Common vertex form factor

$$F_t(q) = \left(\frac{\Lambda_t^2 - m^2}{\Lambda_t^2 - q^2}\right)^2,$$

The only adjustable production parameter

$\Lambda_t = 1.5 \pm 0.2$ GeV

Reggeized propagators

$$\frac{1}{t - m_\pi^2} \to \left(\frac{s}{s_{\text{scale}}}\right)^{\alpha_\pi(t)} \frac{\pi\alpha'_\pi}{\Gamma[\alpha_\pi(t) + 1]\sin[\pi\alpha_\pi(t)]}, \tag{43}$$

$$\frac{1}{t - m_R^2} \to \left(\frac{s}{s_{\text{scale}}}\right)^{\alpha_R(t)-1} \frac{\pi\alpha'_R}{\Gamma[\alpha_R(t)]\sin[\pi\alpha_R(t)]}, \tag{44}$$

the corresponding Regge trajectories for the exchanged mesons are

$$\alpha_R(t) = 1 + \alpha'_R\left(t - m_R^2\right), \qquad R = \rho,\ \omega, \tag{45}$$

$$\alpha_\pi(t) = \alpha'_\pi(t - m_\pi^2), \tag{46}$$

TABLE II: Coupling constants used in this work. The listed three-meson coupling constants are determined by fitting the decay widths from Refs. [20, 23]. The meson-nucleon-nucleon coupling constants entering the lower vertices of the diagrams in Fig. 2 are taken from Ref. [33]. Couplings with mass dimensions are given with explicit units, while those without units are dimensionless.

$g_{K_3^*(1780)\pi K} = 3.84\ \text{GeV}^{-2}$	$g_{K_3^*(1780)\rho K} = 12.36\ \text{GeV}^{-3}$
$g_{K_2(1820)\omega K} = 5.85$	$g_{K_2(1820)\rho K} = 5.70$
$g_{K_2(1770)\omega K} = 5.93$	$g_{K_2(1770)\rho K} = 5.79$
$g_{K^*(1680)\pi K} = 1.76$	$g_{K_4^*(2045)\pi K} = 3.15\ \text{GeV}^{-3}$
$g_{K_3'(2120)\omega K} = 3.02\ \text{GeV}^{-1}$	$g_{K_3'(2120)\rho K} = 2.97\ \text{GeV}^{-1}$
$g_{K_3(1F)\omega K} = 2.71\ \text{GeV}^{-1}$	$g_{K_3(1F)\rho K} = 2.63\ \text{GeV}^{-1}$
$g_{K_2^*(1980)\omega K} = 1.09\ \text{GeV}^{-2}$	$g_{K_2^*(1980)\rho K} = 1.06\ \text{GeV}^{-2}$
$g_{K_2^*(1980)\pi K} = 0.24\ \text{GeV}^{-1}$	$g_{K_5^*(2380)\pi K} = 1.51\ \text{GeV}^{-4}$
$g_{K_4'(1G)\omega K} = 2.13\ \text{GeV}^{-2}$	$g_{K_4(2210)\omega K} = 2.09\ \text{GeV}^{-2}$
$g_{K_3^*(1G)\pi K} = 0.33\ \text{GeV}^{-2}$	

Cross section calculation

The differential cross section in the center-of-mass (c.m.) frame is given by

$$\frac{d\sigma}{d\cos\theta} = \frac{1}{32\pi s}\frac{\left|\vec{k}_2^{\,\text{c.m.}}\right|}{\left|\vec{k}_1^{\,\text{c.m.}}\right|}\left(\frac{1}{2}\sum_{\lambda}|\mathcal{M}|^2\right),$$

The boson propagator can be written as

$$S(p) = \frac{1}{p^2 - M^2}(\not{p} + M)\Delta^{\beta_1\cdots\beta_{n-1}}_{\alpha_1\cdots\alpha_{n-1}}(j,p).$$

The explicit expressions for the projection operators of fields from spin-3 to spin-5 are given as follows

$$\Delta^{\beta}_{\alpha}(1,p) = -\bar{g}^{\beta}_{\alpha} = -\left(g^{\beta}_{\alpha} - \frac{1}{p^2}p_{\alpha}p^{\beta}\right). \qquad \Delta^{\beta_1\beta_2}_{\alpha_1\alpha_2}(2,p) = \frac{1}{2}\left(\bar{g}^{\beta_1}_{\alpha_1}\bar{g}^{\beta_2}_{\alpha_1} + \bar{g}^{\beta_1}_{\alpha_1}\bar{g}^{\beta_1}_{\alpha_2} - \frac{2}{3}\bar{g}_{\alpha_1\alpha_2}\bar{g}^{\beta_1\beta_2}\right).$$

$$\Delta^{\beta_1\beta_2\beta_3}_{\alpha_1\alpha_2\alpha_3}(3,p) = -\frac{1}{36}\sum_{P(\alpha),P(\beta)}\left(\bar{g}^{\beta_1}_{\alpha_1}\bar{g}^{\beta_2}_{\alpha_2}\bar{g}^{\beta_3}_{\alpha_3} - \frac{3}{5}\bar{g}_{\alpha_1\alpha_2}\bar{g}^{\beta_1\beta_2}\bar{g}^{\beta_3}_{\alpha_3}\right)$$

$$\bar{g}_{\mu\nu} = g_{\mu\nu} - \frac{1}{p^2}p_{\mu}p_{\nu}.$$

$$\Delta^{\beta_1\beta_2\beta_3\beta_4}_{\alpha_1\alpha_2\alpha_3\alpha_4}(4,p) = \frac{1}{576}\sum_{P(\alpha),P(\beta)}\left(\bar{g}^{\beta_1}_{\alpha_1}\bar{g}^{\beta_2}_{\alpha_2}\bar{g}^{\beta_3}_{\alpha_3}\bar{g}^{\beta_4}_{\alpha_4} - \frac{6}{7}\bar{g}_{\alpha_1\alpha_2}\bar{g}^{\beta_1\beta_2}\bar{g}^{\beta_3}_{\alpha_3}\bar{g}^{\beta_4}_{\alpha_4} + \frac{3}{35}\bar{g}_{\alpha_1\alpha_2}\bar{g}_{\alpha_3\alpha_4}\bar{g}^{\beta_1\beta_2}\bar{g}^{\beta_3\beta_4}\right),$$

$$= -\left(\frac{1}{120}\right)^2\sum_{P(\alpha),P(\beta)}\left(\bar{g}^{\beta_1}_{\alpha_1}\bar{g}^{\beta_2}_{\alpha_2}\bar{g}^{\beta_3}_{\alpha_3}\bar{g}^{\beta_4}_{\alpha_4}\bar{g}^{\beta_5}_{\alpha_5} - \frac{10}{9}\bar{g}_{\alpha_1\alpha_2}\bar{g}^{\beta_1\beta_2}\bar{g}^{\beta_3}_{\alpha_3}\bar{g}^{\beta_4}_{\alpha_4}\theta^{\beta_5}_{\alpha_5} + \frac{5}{21}\bar{g}_{\alpha_1\alpha_2}\bar{g}_{\alpha_3\alpha_4}\bar{g}^{\beta_1\beta_2}\bar{g}^{\beta_3\beta_4}\bar{g}^{\beta_5}_{\alpha_5}\right),$$

Parameter validation

Total cross section

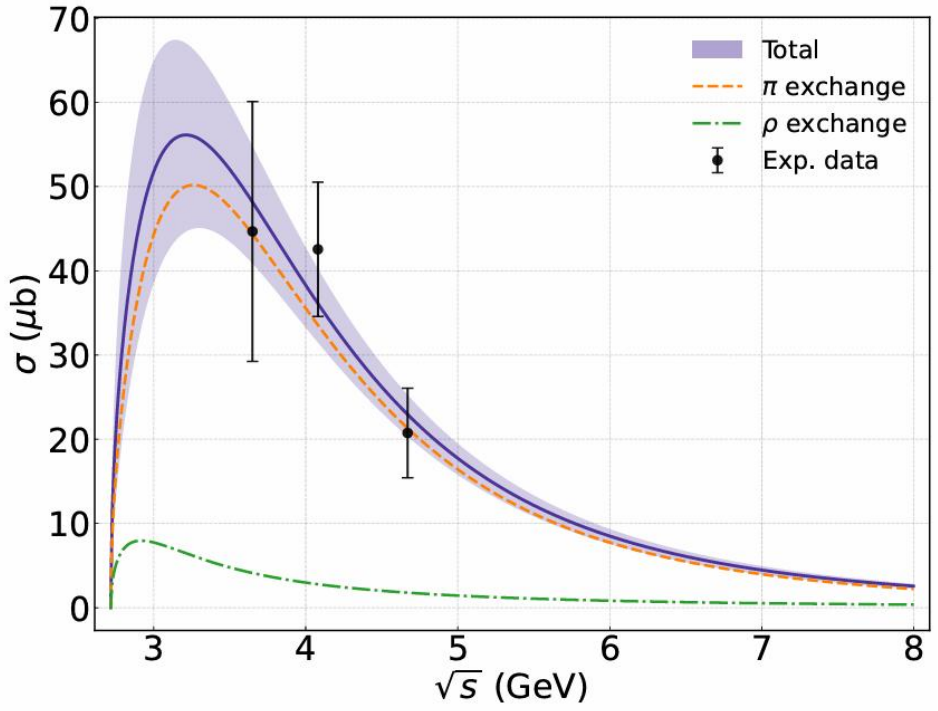


FIG. 3: The calculated total production cross section for the $K_3^*(1780)$ state is presented, along with comparisons to experimental data. The experimental data are taken from Refs. [14–16]. All error bands and the solid lines within them correspond to results obtained with the cutoff parameter set to 1.5 ± 0.2 GeV.

Differential cross section

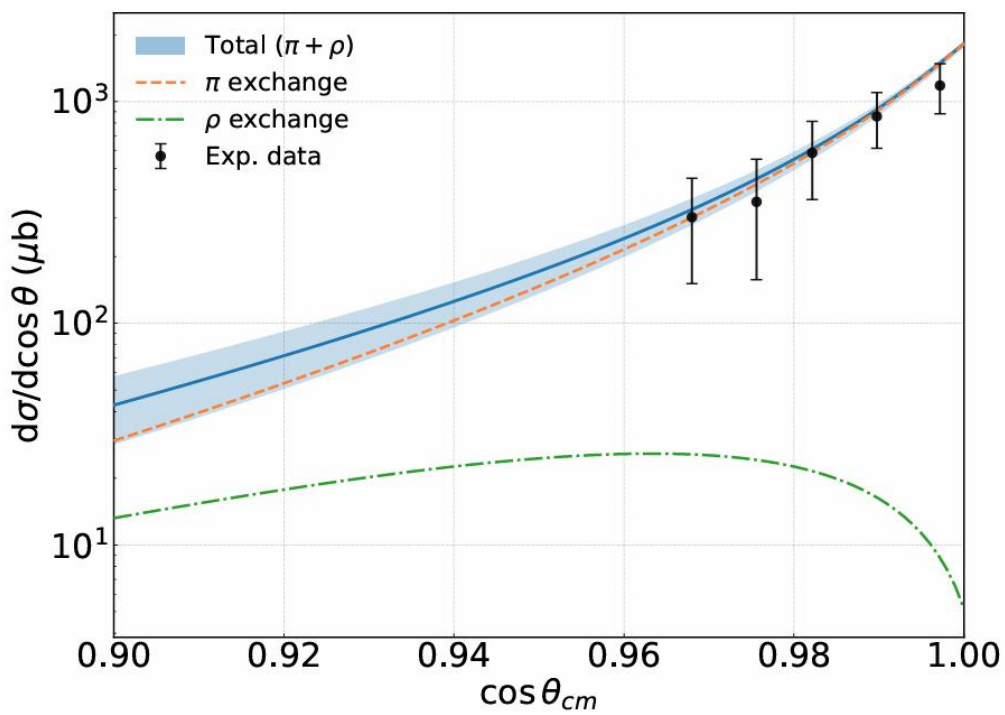
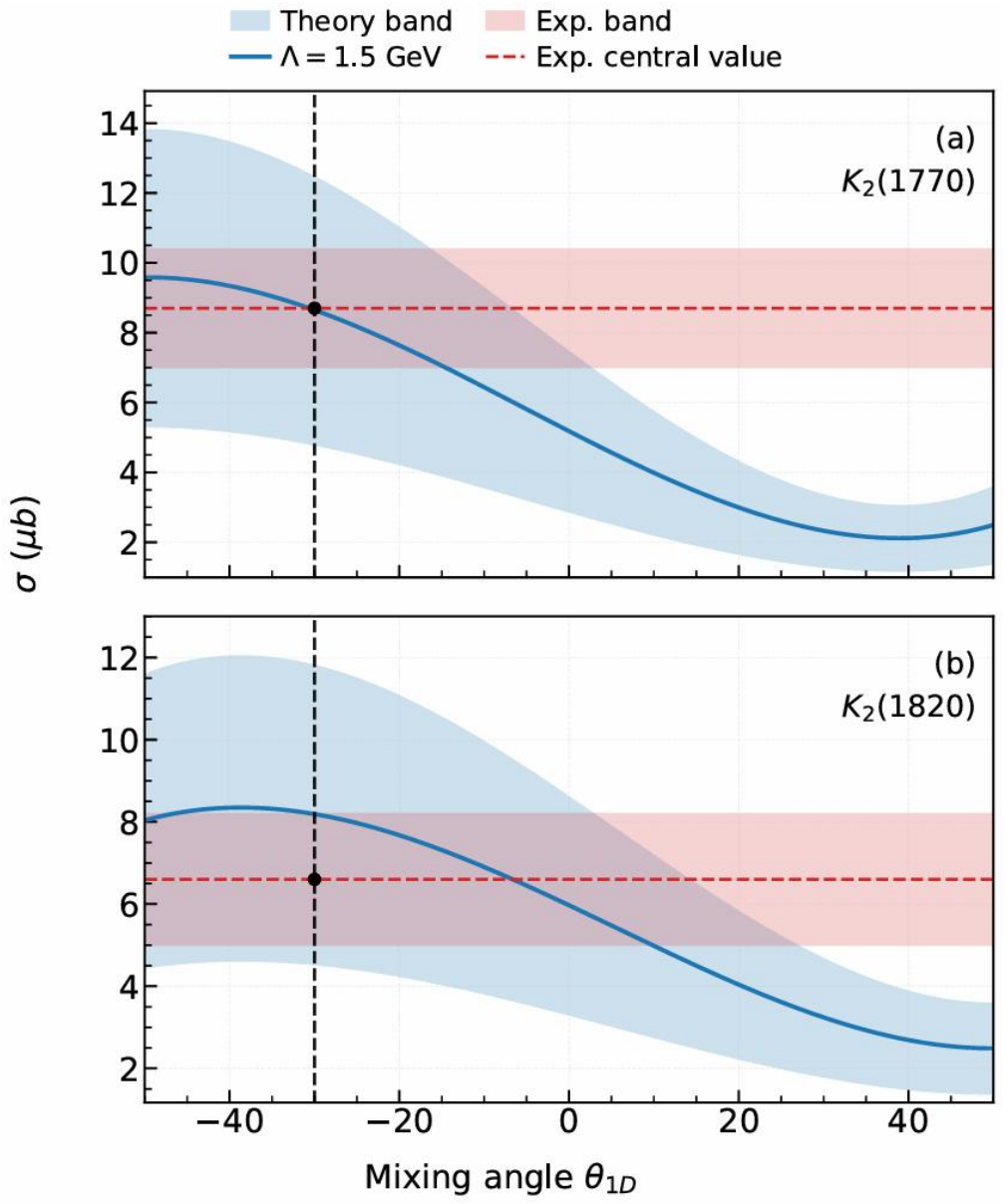


FIG. 4: The calculated differential production cross section for the $K_3^*(1780)$ state is presented, along with comparisons to experimental data. The differential cross section is evaluated at a center-of-mass energy of 4.08 GeV. The experimental data are taken from Ref. [15].

ρ exchange is a small correction. The same Λ_t band also describes the forward distribution at $\sqrt{s}$ = 4.08 GeV.

Production of the two mixed 1D states



$$\begin{pmatrix} |K_2(1770)\rangle \\ |K_2(1820)\rangle \end{pmatrix} \approx \begin{pmatrix} \cos\theta_{1D} & \sin\theta_{1D} \\ -\sin\theta_{1D} & \cos\theta_{1D} \end{pmatrix} \begin{pmatrix} |1^1D_2\rangle \\ |1^3D_2\rangle \end{pmatrix}$$

$K_2(1770)$ **8.7 ± 1.7 μb**

$\sqrt{s}$ = 4.67 GeV

$K_2(1820)$ **6.6 ± 1.6 μb**

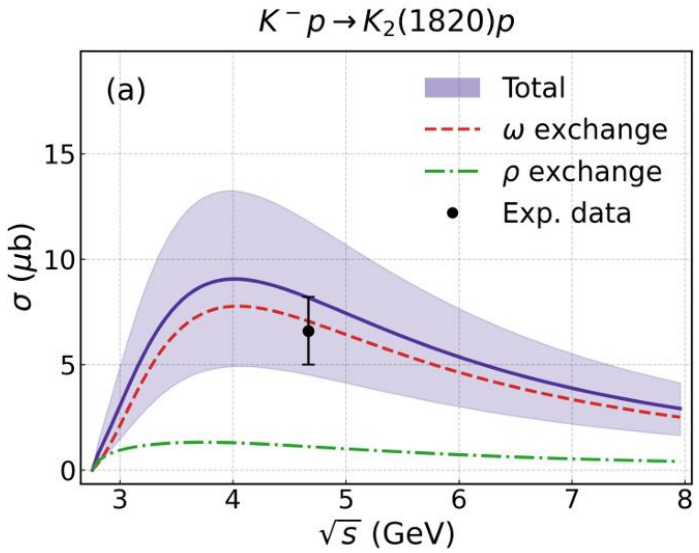
$\sqrt{s}$ = 4.67 GeV

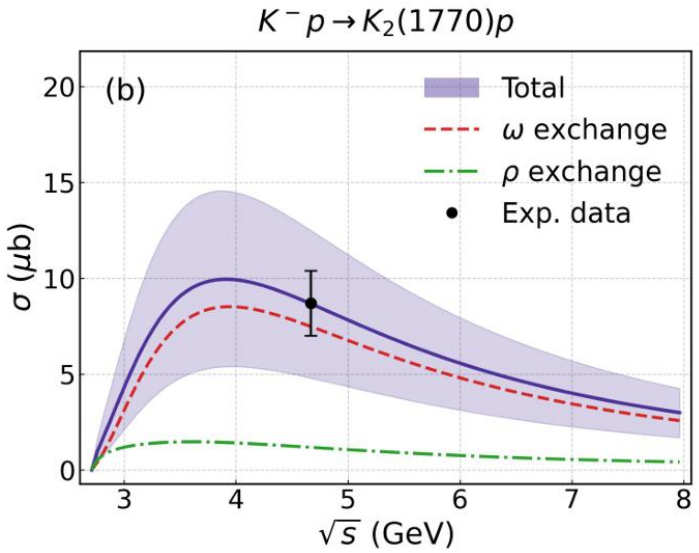
The two states are described by the same mixing angle $\theta_{1D} = -30°$, but their production processes depend on different coupling constants.

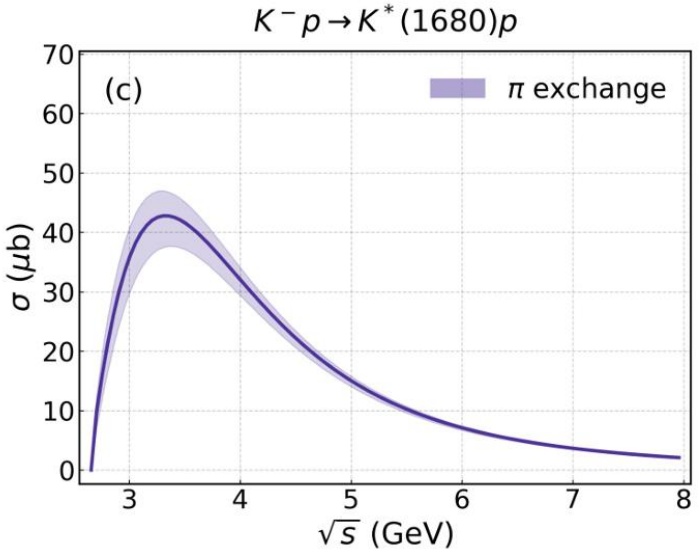
Results for 1D-wave states

Total cross section

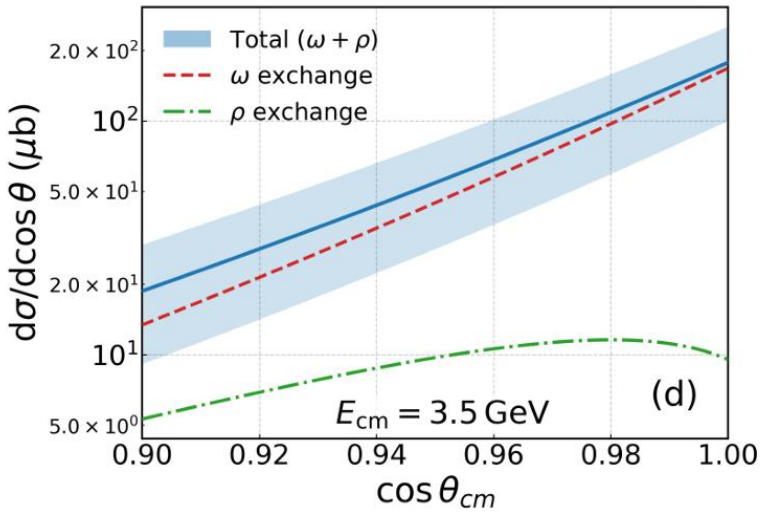
$K_2(1770)$ and $K_2(1820)$ are ω dominated; $K^*(1680)$ is π dominated.
All three channels become strongly forward peaked.

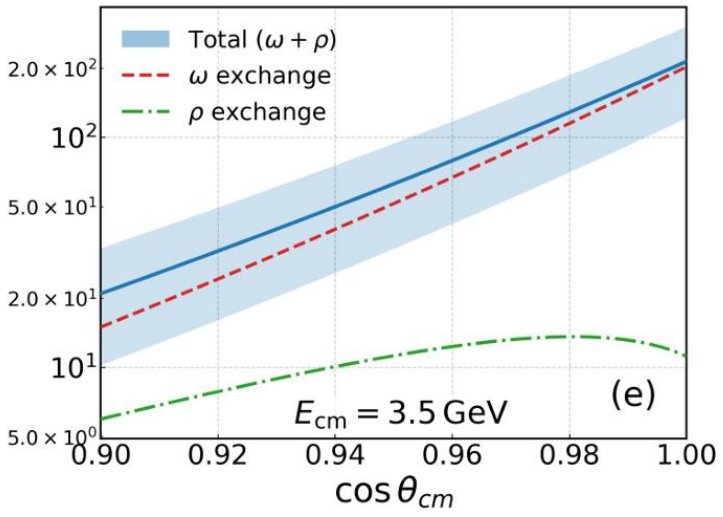


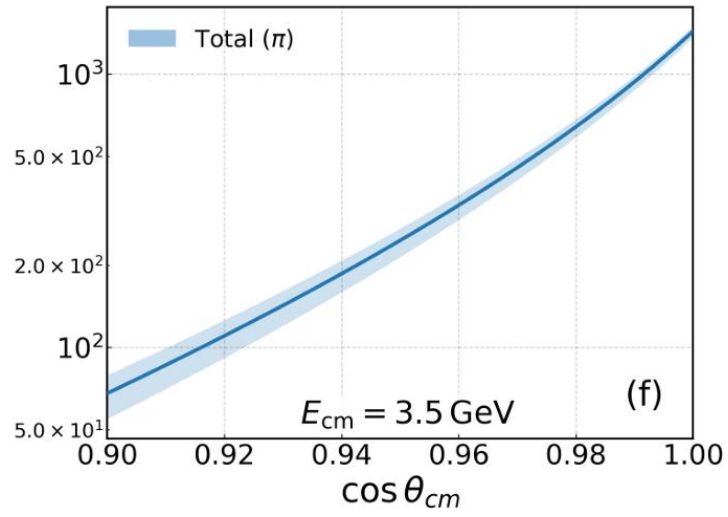




Differential cross section



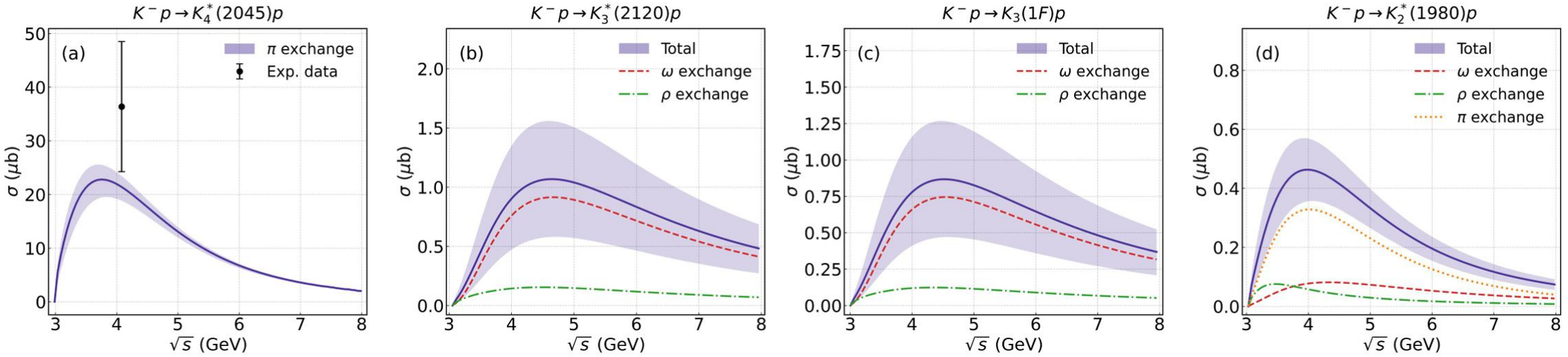




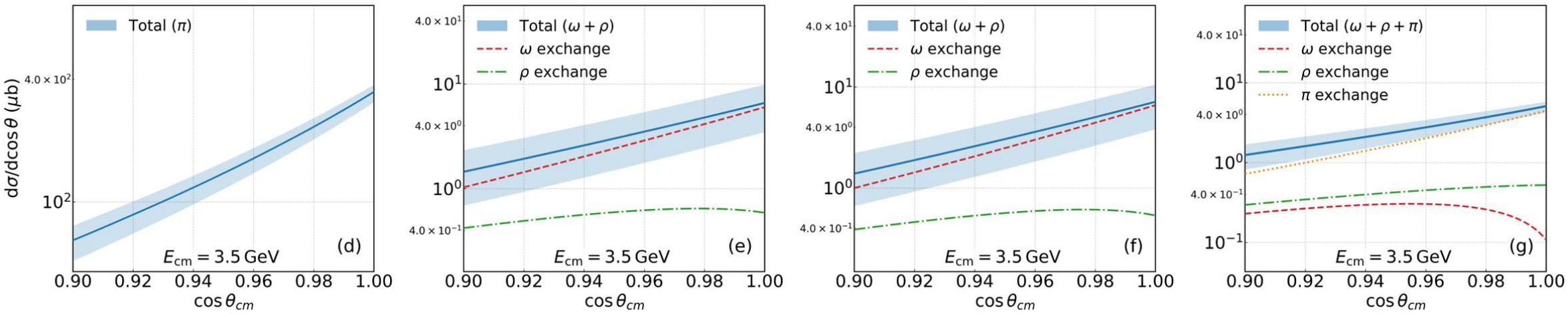
Results for 1F-wave states

Total cross section

Peak values: K_4*(2045) ≈25.6 μb; K_3'(2120) ≈1.1 μb; K_3(1F) ≈0.9 μb; K_2*(1980) ≈0.5 μb.



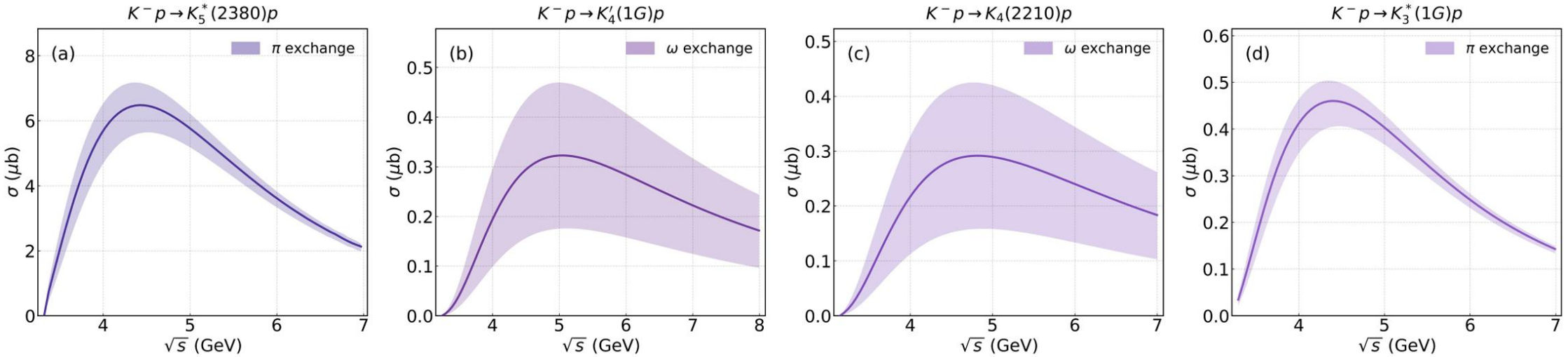
Differential cross section



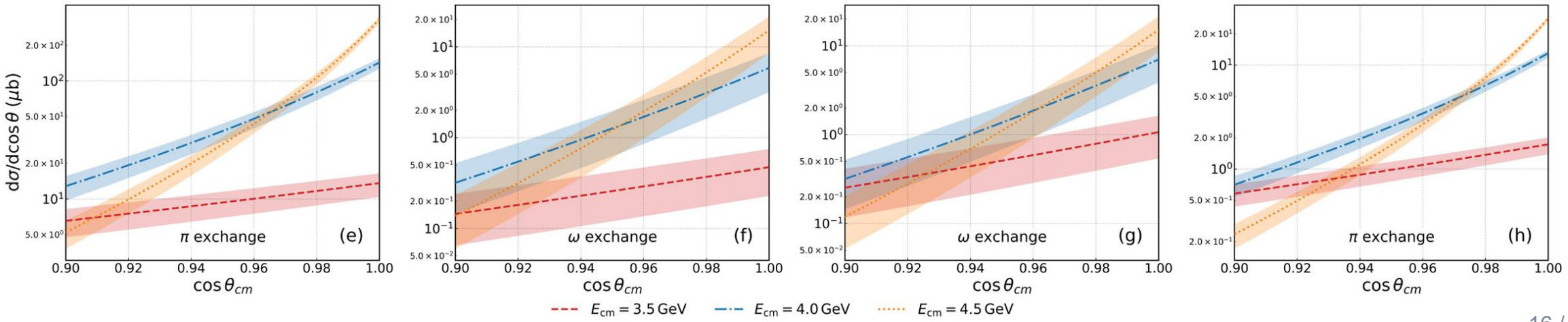
Results for 1G-wave states

Total cross section

Peak values: K_5*(2380) ≈6.5 μb; K_4'(1G) ≈0.32 μb; K_4(2210) ≈0.29 μb; K_3*(1G) ≈0.46 μb.



Differential cross section



Conclusion and outlook

- The same cutoff parameter describes the available production data for several high-orbital kaon states.
- We predict the production cross sections of other high-orbital kaon states using the same model.
- Experiments can search for these states in the invariant-mass spectra of their decay products.

Ting-Yan Li · Lanzhou University

lity2023@lzu.edu.cn | Phys.Rev.D 114 (2026) 3, 034049

Thanks